Dynamic Obstacle Avoidance for Nonholonomic Vehicles using Collision Cones: Theory and Experiments*

Aurora Haraldsen[1], Martin S. Wiig[2], Kristin Y. Pettersen[1,2]

***Abstract*— Obstacle avoidance is a critical part in the control of autonomous vehicles. This paper proposes an obstacle avoidance algorithm based on the computationally advantageous collision cone concept, for unicycles which may be subject to strict input constraints and dynamic, non-compliant obstacles which may even actively pursue a collision. The paper presents both a theoretical analysis together with experiments demonstrating the beneficial features of the algorithm. We analytically derive explicit, and practically intuitive, conditions on the control parameters, under which safety is guaranteed. Experiments illustrate the safe, intuitive, and minimally invasive behaviors generated by the proposed algorithm.**

***Index Terms*— Collision avoidance, nonholonomic systems, reactive algorithms, mobile robots**

I. Introduction

The realization of autonomous vehicles requires advanced guidance, navigation, and control (GNC) systems, where safety is one of the prime concerns. The global path planner can take into account known obstacles and other constraints to produce a safe, feasible, and optimal path, while the reactive controller enables the vehicle to effectively avoid unknown and dynamic obstacles. The main purpose of the latter is thus to provide safety, but without altering the behaviour of the vehicle needlessly. The reactive solution should also regard vehicle dynamics and other factors that could otherwise prevent the fulfillment of the prescribed maneuver.

Methods for reactive collision avoidance include, among others, artificial potential fields (APFs) [1], vector field guidance [2], control barrier functions (CBFs) [3], and geometric methods [4], [5], [6]. APFs have been a staple of reactive collision avoidance for many years, mainly due to its ease of implementation and low computational burden. However, it is well known that the method suffers from local minima and oscillations [7]. CBFs are a more recent development, which can be used to enforce safety of dynamical systems. The idea is to modify the nominal control to satisfy some safety constraints, typically by minimizing the distance between the actual and nominal input subject to the constraints. This requires solving a quadratic programming problem. The relationship between APFs and CBFs was studied in [8], where it was shown that an APF can be formulated as a CBF, and the obtained CBF produced smoother trajectories than the original APF.

APFs were intended for navigation in static environments. Later, some ad-hoc extensions have been proposed for handling dynamic obstacles, but contrary to the traditional APF, these methods are not straight-forward to implement and do not guarantee safety. Similar to APFs, navigation vector fields were proposed for motion planning with static obstacles. Arguably, CBFs present more potential for handling moving obstacles, as they are frequently utilized in multi-agent collision avoidance, see for instance [9], [10], [11], [12]. Safety is concluded based on the assumption that all vehicles follow the same reasoning. However, if a vehicle is non-compliant, a collision will likely occur. Moreover, as indicated in [10], non-hybrid CBFs can in perfectly symmetrical cases result in deadlock situations. If the vehicle has limited control authority, it is also not straight-forward to construct a CBF, as highlighted in [11]. The problem of vanishing control authority is circumvented by so-called synergistic CBFs in [13], which is applied to unicycles with constant speeds for avoiding a static obstacle. [12] proposes a CBF for avoidance of an obstacle moving at a constant velocity, by treating it as an agent with no control inputs. Dynamic obstacles were also considered in [14] for ASVs, but the study similarly assumes that the velocity of an obstacle is constant during the encounter. Moreover, the marine vehicle must be fully actuated in order to employ the proposed CBF scheme and actuator constraints are not considered.

For avoidance of dynamic obstacles, geometric methods present a more straight-forward framework. The concept of collision cones appeared in [15], which constitutes the set of velocities of one point object relative to another point object that will eventually lead to a collision. This notion enables both identification and evasion of collisions in a flexible manner. Furthermore, the underlying strategy is computationally cheap and easily implemented on a wide range of systems. Built on this concept, the velocity obstacle (VO) algorithm [4] was presented for real-time navigation in dynamic environments. The method is based on selecting avoidance maneuvers in the velocity space under a linear acceleration constraint, where the vehicle-obstacle pairs are represented by circular regions. Although the algorithm is computationally advantageous, it relies on the assumption that the velocities are piece-wise constant. The nonlinear velocity obstacle (NLVO) [16] adapts the concept to general

*This work was supported by the Research Council of Norway through project No. 302435 and the Centres of Excellence funding scheme, project No. 223254 – NTNU AMOS.

[1]Aurora Haraldsen and Kristin Y. Pettersen are with the Department of Engineering Cybernetics, Norwegian University of Science and Technology, NO-7491 Trondheim, Norway {Aurora.Haraldsen, Kristin.Y.Pettersen}@ntnu.no

[2]Martin S. Wiig and Kristin Y. Pettersen are with the Norwegian Defence Research Establishment, P.O. Box 25, N-2027 Kjeller, Norway. Martin-Syre.Wiig@ffi.no

(nonlinear) trajectories, in which the VO is comprised by the velocities that would result in a collision given that the current trajectories are maintained. Robot dynamics and constraints are discussed but not formally considered. In [17], the VO is generalized to include the dynamics of a car-like vehicle in a sampling-based algorithm. Here, safety is concluded only if the obstacles move along their current paths, and input constraints are not considered. The acceleration VO (AVO) [18] reformulates the VO to characterize the set of velocities that the vehicle can safely reach under proportional control of the acceleration. Constraints in the applied acceleration are included, but avoidance can only be guaranteed if the obstacle velocity is constant over a chosen time. The related collision cone approach [5] extends the concept to objects of irregular (non-circular) shapes. Vehicle constraints and their inherent limitation on collision avoidance are discussed, however, these are not explicitly considered. [19], [20] extends the method to collision avoidance between quadric surfaces moving in 3D environments, and deforming objects are considered in [21]. Although safety results are presented, they are based on the assumption that the obstacle velocity is at least piece-wise constant and vehicle constraints are not considered. The notion of avoidance maps [22] was proposed for cooperation between multiple UAVs to avoid collisions while moving at constant speeds. The method is based on separating the control effort space into avoiding and colliding regions using the collision cone principle and choosing the lateral acceleration inputs accordingly. The concept is also suggested for non-cooperative collision avoidance, however, without providing any guarantees for success.

Evidently, the majority of existing approaches based on collision cones do not take into account input constraints and/or vehicle dynamics, and obstacles are commonly approximated to move with piece-wise constant velocities. Attempting to bridge some of these gaps, we analyzed the concept when applied to nonholonomic, unicycle-type vehicles with constant speeds and restricted turning rate inputs in [23]. Formal guarantees for safety were derived with respect to these constraints and a circular obstacle with potentially varying speed and direction, thus incorporating more general dynamics of moving objects. This analysis was extended to obstacles of arbitrary shape in [24] and adapted to underactuated surface vessels in [25].

The main contribution of this paper is the extension to unicycles which may also have nonzero accelerations, which was not considered in earlier works, as well as experimental validation of the proposed algorithm. Since many vehicles must adhere to strict acceleration constraints, we choose to not use the acceleration input actively to avoid collision but consider it a possible disturbance in the collision avoidance control, which provides a large amount of flexibility in the speed and acceleration control of the vehicle. Moreover, the vehicle kinematics and additional input constraints are considered in an analysis of the algorithm, wherein we derive explicit requirements for safety. Contrary to most previous studies, the obstacle is modeled as a kinematic vehicle capable of changing both its speed and direction at any instant. The proposed method is validated experimentally on two mobile robots in the Robotarium [26], which demonstrates the performance under real conditions.

The remainder of the paper is organized as follows. The control model and problem are outlined in Section II, and the heading controller for steering the vehicle in the correct direction is presented in Section III. The guidance system is described in the two following parts, where Section IV states the nominal guidance law applied to make the vehicle move towards a goal destination and Section V presents the collision avoidance strategy. In Section VI, we provide a mathematical analysis of the avoidance problem and proposed solution. The results from the experimental study is presented in Section VII, before some concluding remarks are given in Section VIII.

II. Problem Statement

The vehicle and the obstacle are modeled as nonholonomic unicycles with bounded inputs:

$$\dot{x} = u\cos(\psi), \tag{1a}$$
$$\dot{y} = u\sin(\psi), \tag{1b}$$
$$\dot{\psi} = r, \qquad r \in [-r^{\max}, r^{\max}], \tag{1c}$$
$$\dot{u} = a, \qquad a \in [-a^{\max}, a^{\max}], \tag{1d}$$

where x, y are the Cartesian coordinates, ψ and r are the heading angle and heading rate, respectively, and u and a are the forward speed and acceleration. Moreover, $r^{\max}$ and $a^{\max}$ are constant, non-negative parameters. The state of the system is collected as $\boldsymbol{x} \triangleq [x, y, \psi, u]^T$, and we use the notation $\boldsymbol{p} \triangleq [x,\ y]^T$ and $\boldsymbol{v} \triangleq \dot{\boldsymbol{p}}$. The subscript o is employed to separate the obstacle system from the vehicle to this end.

To account for the physical areas, we define that a collision occurs when the distance between the vehicle and the obstacle, $d \triangleq \|\boldsymbol{p} - \boldsymbol{p}_o\|$, is reduced to less than a minimum distance, $d^{\min} > 0$, rather than when they attain the same position. To stay safe, the vehicle should thus remain in the safe set

$$\mathcal{C}^{\text{safe}} \triangleq \{\, \boldsymbol{x} \,:\, \|\boldsymbol{p} - \boldsymbol{p}_o\| \geq d^{\min} \,\}. \tag{2}$$

In addition to collision avoidance, we require that the vehicle comes within an acceptable distance, $d^{\text{acc}} > 0$, of a target position $\boldsymbol{p}_{\text{t}}$. Hence, the vehicle should reach the goal set

$$\mathcal{C}^{\text{goal}} \triangleq \{\, \boldsymbol{x} \,:\, \|\boldsymbol{p} - \boldsymbol{p}_{\text{t}}\| \leq d^{\text{acc}} \,\}. \tag{3}$$

The control problem can thus be summarized as the achievement of the following objectives:

$$\boldsymbol{x}(t) \in \mathcal{C}^{\text{safe}}(t), \forall t \geq t_0 \tag{4}$$
$$\lim_{t\to\infty} \boldsymbol{x}(t) \in \mathcal{C}^{\text{goal}}(t). \tag{5}$$

III. Speed and Heading Control

In Sections IV-V we will present the guidance system that generates the heading direction, ψ_{d}, the vehicle should

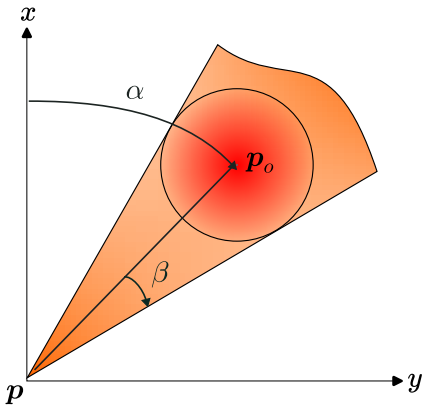

Fig. 1: Collision cone.

follow to achieve the aforementioned objectives. To make the vehicle keep the desired heading, we apply the controller

$$r = \begin{cases} r^{\max} & \text{if } \tilde{\psi} > 0, \\ 0 & \text{if } \tilde{\psi} = 0, \\ -r^{\max} & \text{if } \tilde{\psi} < 0, \end{cases} \tag{6}$$

where the angular difference $\tilde{\psi} \triangleq -(\psi - \psi_{\mathrm{d}})$ is mapped to the interval $\tilde{\psi} \in (-\pi, \pi]$ to ensure that the vehicle always takes the shortest turn. This will make the vehicle exert maximum control power to reach the commanded heading.

Assumption 1. The forward speed of the vehicle satisfies

$$u \in \left[u^{\min}, u^{\max}\right], \tag{7}$$

where $u^{\max}, u^{\min} > 0$ are constant parameters,

Remark 1. Although the speed of the vehicle can be controlled through the acceleration input, the proposed avoidance strategy does not require the vehicle to accelerate. Since the vehicle looses controllability when $u = 0$, Assumption 1 is a required but mild assumption. The algorithm can thus be combined with most onboard speed control schemes. An additional requirement on the speed will be stated in Section V.

IV. Target Reaching

To steer the vehicle towards the target destination $\boldsymbol{p}_{\mathrm{t}}$, we will use a pure pursuit guidance law [27] to compute the desired velocity of the vehicle. For static targets such as the one we are considering, this method will make the vehicle take the shortest path to the target. The guidance law is based on aligning the vehicle velocity with the line-of-sight vector from the vehicle to the target. For vehicles modeled on the form (1), the guidance strategy requires the vehicle to keep a heading direction given by

$$\psi_{\mathrm{pp}} \triangleq \operatorname{atan2}(y_{\mathrm{t}} - y, x_{\mathrm{t}} - x). \tag{8}$$

Hence, to make the vehicle move to the target position, we set the desired heading equal to $\psi_{\mathrm{d}} = \psi_{\mathrm{pp}}$. In the next section, we present the theory and resulting logic that determines when the vehicle must deviate from (8) in order to stay in the safe set.

V. Collision Avoidance

While moving towards the target, the vehicle may need to adjust its heading to avoid the obstacle. A collision cone is therefore employed to identify potential collisions and make the necessary adjustments to the trajectory. As discussed in the Introduction, we do not utilize the acceleration input in the collision avoidance control, as the evasive maneuvers are based purely on a change of direction. However, acceleration effects are considered in the analysis given in Section VI. Hence, the algorithm can safely be applied to vehicles with limited acceleration capabilities, but also to vehicles that accelerate more actively. We demonstrate this flexibility in the experimental study presented in Section VII.

A. Conflict Detection

If the vehicle and the obstacle move indefinitely in their current directions, they must end up in a collision if the relative velocity, $\boldsymbol{v} - \boldsymbol{v}_o$, is directed towards the circular region in Figure 1. The *collision cone* corresponds to the orange area in Figure 1, characterizing the set of velocities leading to a future collision. The orientation of the right and left cone vertex can be found respectively as

$$\alpha \pm \beta, \tag{9}$$

where $\alpha \triangleq \operatorname{atan2}(y_o - y, x_o - x)$ represents the orientation of the line-segment going from $\boldsymbol{p}$ to $\boldsymbol{p}_o$ and

$$\beta \triangleq \begin{cases} \sin^{-1}\left(\frac{d^{\min}}{d}\right) & \text{if } d \geq d^{\min}, \\ \pi - \sin^{-1}\left(\frac{d}{d^{\min}}\right) & \text{otherwise,} \end{cases} \tag{10}$$

represents the half-width angle of the cone. Notice that this definition also includes the case in which the vehicle is not in the safe set. Although such a situation should be avoided entirely according to the objective (4), the second part of (10) is included for the purpose of the first lemma which provides sufficient conditions for convergence to the safe set as well as forward invariance of this set.

Lemma 1. *Consider an obstacle moving with the time-varying velocity $\boldsymbol{v}_o$, and let the vehicle maintain a time-varying velocity $\boldsymbol{v}$ satisfying*

$$|\chi(t) - \alpha(t)| = \beta(t), \quad \forall\, t \geq t_1, \tag{11}$$

where $\chi \triangleq \operatorname{atan2}(\dot{y} - \dot{y}_o, \dot{x} - \dot{x}_o)$ is the relative direction of the vehicle with respect to the obstacle, for some time $t_1 \geq t_0$. Then, the vehicle will converge to the boundary of the safe set (2)*, that is*

$$\lim_{t \to \infty} \boldsymbol{x}(t) = \partial \mathcal{C}^{\mathrm{safe}}(t). \tag{12}$$

Furthermore, if $\boldsymbol{x}(t_1) \in \mathcal{C}^{\mathrm{safe}}(t_1)$ and the vehicle maintains a velocity satisfying

$$|\chi(t) - \alpha(t)| \geq \beta(t), \quad \forall\, t \geq t_1, \tag{13}$$

then the vehicle will remain in the safe set, that is

$$\boldsymbol{x}(t) \in \mathcal{C}^{\mathrm{safe}}(t), \quad \forall\, t \geq t_1. \tag{14}$$

Proof: The time-derivative of the distance d can be found geometrically as

$$\dot{d} = -\|\boldsymbol{v} - \boldsymbol{v}_o\| \cos(\chi - \alpha). \tag{15}$$

With (11), the time-derivative of the distance is given by

$$\dot{d} = \begin{cases} -\|\boldsymbol{v} - \boldsymbol{v}_o\| \sqrt{1 - \left(\frac{d^{\min}}{d}\right)^2} & \text{if } d \geq d^{\min}, \\ \|\boldsymbol{v} - \boldsymbol{v}_o\| \sqrt{1 - \left(\frac{d}{d^{\min}}\right)^2} & \text{otherwise,} \end{cases} \tag{16}$$

where we see that if $d < d^{\min}$, then $\dot{d} > 0$, and if $d > d^{\min}$, then $\dot{d} < 0$. Finally, if $d = d^{\min}$, $\dot{d} = 0$. Hence, the vehicle converges to the boundary of the safe set, where $d = d^{\min}$. If (13) holds, the time-derivative of d satisfies

$$\dot{d} \geq -\|\boldsymbol{v} - \boldsymbol{v}_o\| \sqrt{1 - \left(\frac{d^{\min}}{d}\right)^2}, \quad \forall\, d \geq d^{\min}. \tag{17}$$

Since $\dot{d} \geq 0$ on the boundary of $\mathcal{C}^{\text{safe}}$, the set is positively invariant. Hence, any trajectory starting in it cannot leave, which concludes the proof. ∎

A situation where the vehicle does not satisfy the condition (13) will be called a conflict. If the obstacle comes too close to the vehicle during a conflict, then the vehicle should take action to avoid a collision. This strategy will be formalized in the next section.

B. Conflict Prevention and Resolution

In order to construct an evading maneuver, it is convenient to express the collision cone in terms of the absolute vehicle heading. This is done by first translating the collision cone by the obstacle velocity, $\boldsymbol{v}_o$, as illustrated in Figure 2. The shifted cone, given in yellow, characterizes the set of absolute velocities that will result in a collision with the obstacle, corresponding to the *velocity obstacle* of [4]. The angles at which the velocity of the vehicle is directed inside of this set is then given by the intersections between the circle of radius equal to the magnitude of the vehicle velocity, $\boldsymbol{v}$, and this cone, represented by the dashed lines in Figure 2. Analytical expressions for these angles can be found as

$$\psi_{\text{cc}}^{\pm} \triangleq \alpha \pm \beta + \gamma^{\pm}, \tag{18}$$

where the angle γ is derived geometrically as

$$\gamma^{\pm} \triangleq \sin^{-1}\left(\frac{u_o}{u} \sin\left(\lambda^{\pm}\right)\right), \tag{19}$$

and we define $\lambda^{\pm} \triangleq \pi - \psi_o + \alpha \pm \beta$ for conciseness.

It can be noticed that the angles $\gamma^{\pm}$ are not always defined. In such cases, an avoidance maneuver may not exist. Although it is possible to deal with this by an appropriate choice of the input acceleration, we consider the more general case where the maximum acceleration may be zero. Another way to handle this is by requiring that the following assumption holds:

Assumption 2. The speed of the obstacle is bounded by

$$u_o \in [0, u_o^{\max}], \tag{20}$$

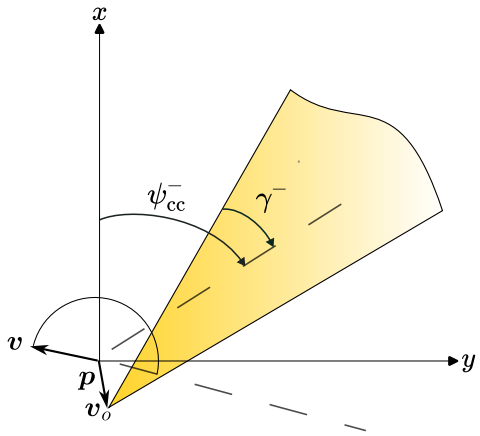

Fig. 2: Geometric representation of the angles ψ_{cc}^{-} and γ^{-}.

where $0 \leq u_o^{\max} < u^{\min}$ is a constant parameter.

Remark 2. Assumption 2 requires that the speed of the obstacle is bounded, which is easily justified. However, it also implies that the vehicle keeps a higher speed than the obstacle. We note that the last part only has to be satisfied in a close vicinity of the obstacle. This will enable a swift and secure evasion, even if the obstacle should actively pursue a collision.

To ensure that the avoidance control is strictly necessary, the distance to the obstacle should be reduced to a critical distance, $d^{\text{crit}} > 0$, before an avoiding maneuver is performed. Therefore, only if the nominal heading (8) places the vehicle and the obstacle in conflict by the condition

$$|\chi - \alpha| < \beta, \tag{21}$$

and the distance satisfies $d \leq d_{\text{crit}}$, then the control system will initiate a conflict resolving maneuver by assigning the heading $\psi_{\text{d}} = \psi_{\text{ca}}^{j}$, with

$$\psi_{\text{ca}}^{\pm} \triangleq \psi_{\text{cc}}^{\pm} \pm \epsilon, \tag{22}$$

where $\epsilon > 0$ is a constant parameter that can be considered as an adjustable safety margin. Moreover, the direction of the heading change is expressed by j. This parameter determines which side of the obstacle the vehicle attempts to pass on. A safe option is to choose

$$j = \underset{j \in \{\pm\}}{\text{argmax}} \begin{cases} \left|\psi_o - \psi_{\text{cc}}^{j}\right| & \text{if } d = d^{\text{crit}} \\ -\left|\psi - \psi_{\text{cc}}^{j}\right| & \text{otherwise,} \end{cases} \tag{23}$$

where we assume that the angular difference is mapped to the interval $(-\pi, \pi]$. Note that in the first case of (23), both directions will guarantee evasion provided that the critical distance is set accordingly. The second case of (23) ensures that the vehicle is always turning away from a conflict that has not yet occurred.

Once the nominal velocity does not lead to a conflict according to (21), we reassign the desired heading to

$$\psi_{\text{d}} = \psi_{\text{pp}}. \tag{24}$$

VI. Analysis

Lemma 1 showed geometrically that the vehicle and the obstacle cannot collide unless they are currently in a conflict. Define as in [28] the angular distances to a conflict:

$$\delta^{\pm} \triangleq \pm\psi \mp \psi_{\text{cc}}^{\pm}, \tag{25}$$

corresponding to a clockwise and counterclockwise turn, respectively. If the linear distance to the obstacle is less than the critical distance, d^{crit}, the algorithm is designed to prevent a potential conflict by making the vehicle adjust its orientation according to the collision cone of the obstacle. However, since the vehicle is subject to turning constraints, we need an additional condition in order to guarantee that the required maneuver is fulfilled, derived in the next lemma.

Lemma 2. *Consider an obstacle and a vehicle modeled by* (1)*. Let Assumptions 1-2 hold. Suppose that the vehicle and the obstacle at some time $t_1 \geq t_0$ are not in a conflict, i.e.*

$$|\chi(t_1) - \alpha(t_1)| \geq \beta(t_1), \tag{26}$$

and $\boldsymbol{x}(t_1) \in \mathcal{C}^{\text{safe}}(t_1)$. Then, a control input r satisfying

$$\begin{aligned} \delta^{+} = 0 \Rightarrow r = r^{\max}, \\ \delta^{-} = 0 \Rightarrow r = -r^{\max}, \end{aligned} \tag{27}$$

where

$$r^{\max} \geq r_o^{\max}\frac{u_o^{\max}}{u^{\min}} + \frac{a_o^{\max}u^{\min} + a^{\max}u_o^{\max}}{u^{\min}\sqrt{u^{\min 2} - u_o^{\max 2}}}, \tag{28}$$

will keep the vehicle out of conflict with the obstacle for all future time, that is

$$|\chi(t) - \alpha(t)| \geq \beta(t), \quad \forall\, t \geq t_1, \tag{29}$$

Proof: The angular distances (25) are defined such that they are non-negative, $\delta^{\pm} \geq 0$, when the vehicle is not in conflict with the obstacle. Define the set $\mathcal{C}^{\delta} = \{\boldsymbol{x} : \delta^{\pm} \geq 0\}$. The set is positively invariant if $\dot{\delta}^{\pm} \geq 0, \forall\, \boldsymbol{x} \in \partial\mathcal{C}^{\delta}$, where $\partial\mathcal{C}^{\delta} = \{\boldsymbol{x} : \delta^{\pm} = 0\}$ denotes the boundary of the set. On $\partial\mathcal{C}^{\delta}$, the time-derivative of (25) is computed as

$$\dot{\delta}^{\pm} = \pm r \mp \dot{\alpha} - \dot{\beta} \mp \dot{\gamma}^{\pm}. \tag{30}$$

The time-derivative of $\gamma^{\pm}$ is

$$\begin{aligned} \dot{\gamma}^{\pm} = (-r_o + \dot{\alpha} \pm \dot{\beta})\frac{u_o\cos(\lambda^{\pm})}{\sqrt{u^2 - u_o^2\sin^2(\lambda^{\pm})}} \\ + a_o\frac{\sin(\lambda^{\pm})}{\sqrt{u^2 - u_o^2\sin^2(\lambda^{\pm})}} - a\frac{u_o\sin(\lambda^{\pm})}{u\sqrt{u^2 - u_o^2\sin^2(\lambda^{\pm})}}. \end{aligned} \tag{31}$$

Furthermore, $\dot{\alpha}$ is found geometrically as

$$\dot{\alpha} = -\frac{\|\boldsymbol{v} - \boldsymbol{v}_o\|}{d}\sin(\chi - \alpha), \tag{32}$$

and the time-derivative of β is computed from (10) as

$$\dot{\beta} = \frac{\|\boldsymbol{v} - \boldsymbol{v}_o\|}{d}\cos(\chi - \alpha)\tan(\beta). \tag{33}$$

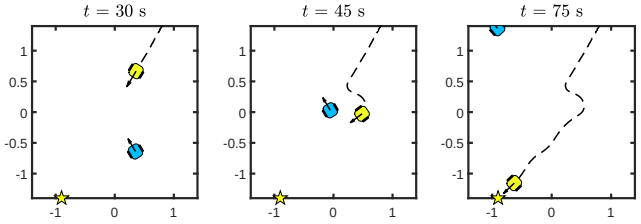

(a) Snapshots from the experiment, where the main robot is marked in yellow and the obstacle robot in blue. The goal position is represented by the star, and the trajectory of the main robot is given by the dashed line.

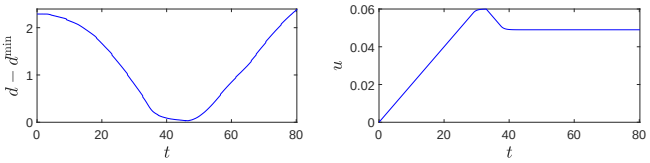

(b) Distance and commanded speed during the experiment.

Fig. 3: Results from the first experiment.

Hence, $\dot{\beta} \pm \dot{\alpha} = 0$ when $\delta^{\pm} = 0$ (since then $\chi = \alpha \pm \beta$), and

$$\begin{aligned} \dot{\delta}^{\pm} = \pm r \pm r_o\frac{u_o\cos(\lambda^{\pm})}{\sqrt{u^2 - u_o^2\sin^2(\lambda^{\pm})}} \\ \mp a_o\frac{\sin(\lambda^{\pm})}{\sqrt{u^2 - u_o^2\sin^2(\lambda^{\pm})}} \pm a\frac{u_o\sin(\lambda^{\pm})}{u\sqrt{u^2 - u_o^2\sin^2(\lambda^{\pm})}}. \end{aligned} \tag{34}$$

Under the model (1) and Assumptions 1-2, (34) is bounded:

$$\dot{\delta}^{\pm} \geq \pm r - r_o^{\max}\frac{u_o^{\max}}{u^{\min}} - \frac{a_o^{\max}u^{\min} + a^{\max}u_o^{\max}}{u^{\min}\sqrt{u^{\min 2} - u_o^{\max 2}}}. \tag{35}$$

It follows that $\dot{\delta}^{\pm} \geq 0, \forall\, \boldsymbol{x} \in \partial\mathcal{C}^{\delta}$ when the control input satisfies (27) and the maximum rate is lower bounded by (28). Since $\mathcal{C}^{\delta}$ is positively invariant, any trajectory starting in the set cannot leave it. Hence, (29) holds. ■

Remark 3. The relation (34) shows that the acceleration can be used to prevent a conflict rather than cause one, by treating a as an input instead of an arbitrary disturbance as we do here. This would require a more advanced control logic, which is left for future work.

We will conclude this section by stating the main theorem, which presents the complete set of conditions ensuring achievement of the control objectives (4)-(5). The last assumption implies that the obstacle cannot block the target:

Assumption 3. The obstacle keeps at least a distance d^{crit} to the target position $\boldsymbol{p}_{\text{t}}$, that is

$$\|\boldsymbol{p}_o(t) - \boldsymbol{p}_{\text{t}}\| \geq d^{\text{crit}}, \quad \forall\, t \geq t_0. \tag{36}$$

Remark 4. Assumption 3 is a formality and does not have to hold for all time, but rather after a certain point. This is to allow the vehicle to move towards the target without being at constant risk of collision, as this could make the vehicle stuck.

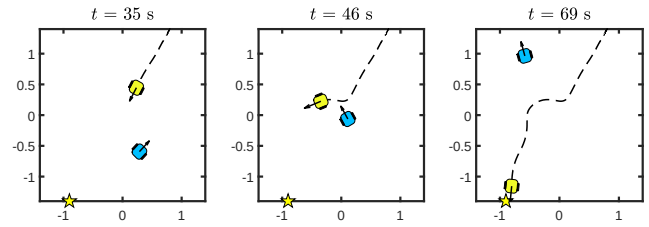

(a) Snapshots from the experiment.

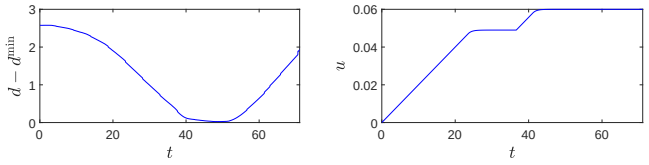

(b) Distance and commanded speed during the experiment.

Fig. 4: Results from the second experiment.

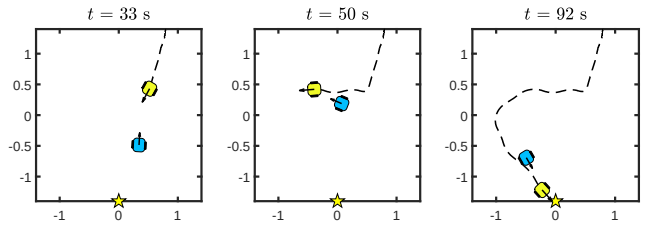

(a) Snapshots from the experiment.

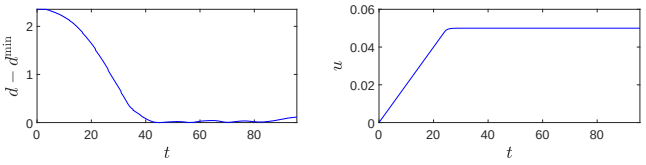

(b) Distance and commanded speed during the experiment.

Fig. 5: Results from the third experiment.

Theorem 1. *Consider an obstacle and a vehicle modeled by* (1)*. Let Assumptions 1-3 hold and the initial distance satisfy* $d(t_0) \geq d^{\text{crit}}$*. Furthermore, let the critical distance satisfy*

$$d^{\text{crit}} \geq \frac{2u^{\max} + \pi u_o^{\max}}{r^{\max}} + d^{\min}, \tag{37}$$

the acceptance distance satisfy

$$d^{\text{acc}} \geq \frac{u^{\max}}{r^{\max}}, \tag{38}$$

and the maximum heading rate satisfy condition (28) *of Lemma 2. Then, the vehicle with the heading controller* (6)*, the pure pursuit guidance law* (8)*, and the collision avoidance algorithm* (21) - (24)*, will reach within the acceptable distance of the target position* $\boldsymbol{p}_{\text{t}}$ *without collision.*

Proof: The proof follows the same line of arguments as the proof of [23, Theorem 2]: If there is a conflict as the distance is reduced to the critical distance, the lower bound (37) ensures that the vehicle has time to resolve it before the obstacle can make the vehicle leave the safe set. By Lemma 2, the vehicle will prevent a conflict by keeping the avoidance heading (22) with the heading controller (6) if the nominal direction is conflicting while $d < d^{\text{crit}}$. Hence, the vehicle stays in the safe set by Lemma 1. Since the vehicle maintains a speed satisfying Assumption 2, the vehicle will eventually escape the obstacle. The lower bound (38) ensures that the vehicle reaches the goal set (3) under the guidance law (8) and the constraints of the model (1) [29]. ■

VII. Experimental Results

In this section, we validate the algorithm using two mobile robots in the Robotarium [26], where one of the robots, referred to as the main or vehicle robot, follows the avoidance algorithm towards a goal position, while the second robot acts as a dynamic obstacle and thus moves around freely. The robots have a radius of 11 cm and the test bed has an area of 3.2×2 m^2. The linear maximum speed of the robots is 20 cm/s and the maximum rotation speed is 3.6 rad/s. The motors of the robots are restricted to only rotate at a maximum speed of 12.5 rad/s, which limits the simultaneous linear and rotational speed of the robots accordingly. In all tests, the robots were first commanded to an initial pose, from where the actual experiment was conducted. The maximum speed of the obstacle robot was set to $u_o^{\max} = 4.8$ cm/s, and the maximum angular velocity and forward acceleration were set to $r_o^{\max} = 0.5$ rad/s and $a_o^{\max} = 0.2$ cm/s^2, respectively. The minimum vehicle speed was set according to Assumption 2 as $u^{\min} = 4.9$ cm/s, and the maximum speed was chosen as $u^{\max} = 6$ cm/s. The maximum angular velocity was selected as $r^{\max} = 0.9$ rad/s and the maximum linear acceleration as $a^{\max} = 0.2$ cm/s^2, such that the condition (28) holds. The minimum required distance was chosen to be $d^{\min} = 50$ cm in order to leave some extra space around the robots, and the critical distance was set to $d^{\text{crit}} = 1$ m in accordance with the lower bound (37). The acceptance distance was chosen to comply with (38) as $d^{\text{acc}} = 10$ cm, and we chose $\epsilon = 5$ degrees.

In the first test, the vehicle is commanded to the target position $\boldsymbol{p}_{\text{t}} = [-0.9, -1.4]^\top$ m at the maximum forward speed. The results are plotted in Figure 3. The obstacle robot can be seen to cross in front of the vehicle robot, causing it to take a right turn in accordance with (23). The forward speed of the main robot is simultaneously reduced to the minimum. The main robot passes behind the obstacle robot and continues to the goal destination, during which the distance is kept above the minimum distance at all times, as verified by Figure 3b.

In the second experiment, shown in Figure 4, the vehicle is commanded to the same position as in the previous test at the minimum forward speed. The obstacle robot passes on the left side of the vehicle robot but subsequently changes direction. The main robot is then forced to move to the side in order to avoid the other robot. During this situation, the speed of the vehicle robot is increased to the maximum as shown in Figure 4b. The robot avoids the collision by following the avoidance strategy and then converges to the target position.

In the third experiment, we demonstrate the algorithm in

a more threatening scenario, where the obstacle robot is to pursue a collision by tracking the main vehicle. The robots were initialized on opposite sides, from where the main robot was to reach a goal point close to the starting point of the obstacle robot. The commanded forward speed was in this case constant and given by 5 cm/s. As shown in Figure 5a, the obstacle robot creates a potential collision, and the main robot takes a turn to avoid it. The vehicle keeps turning as required until it escapes the pursuing robot and proceeds to the target. From Figure 5b, it can be verified that the required distance between the robots is kept under the full encounter.

VIII. Conclusions and Future Work

In this paper, we have presented the analysis and experimental validation of a reactive obstacle avoidance method which is suitable for vehicles with unicycle kinematics that may be subject to strict acceleration constraints and may have limited turning rates. The algorithm utilizes the computationally advantageous collision cone notion to effectively determine when a collision is impending and produce an immediate evasion, without the need for controlling the forward acceleration of the vehicle. Explicit conditions on the speed and turning rate of the vehicle were derived through a mathematical analysis of the closed-loop system, guaranteeing safety in any encounter with a dynamic, non-compliant obstacle. Minimum requirements on the parameters of the algorithm were presented for the achievement of a nominal goal. The approach was verified experimentally on mobile robots in the Robotarium, demonstrating the resulting vehicle behaviour in different encounters with a moving obstacle.

Future work involves exploiting the acceleration input of the vehicle for collision avoidance. It also concerns exploring other models of the dynamic environment and consider factors such as measurement uncertainties.

References

[1] O. Khatib, "Real-time obstacle avoidance for manipulators and mobile robots," in *Proc. IEEE International Conference on Robotics and Automation*, 1985, pp. 500–505.

[2] D. Panagou, "Motion planning and collision avoidance using navigation vector fields," in *Proc. IEEE International Conference on Robotics and Automation*, 2014, pp. 2513–2518.

[3] A. D. Ames, S. Coogan, M. Egerstedt, G. Notomista, K. Sreenath, and P. Tabuada, "Control barrier functions: Theory and applications," in *Proc. 18th European Control Conference*, 2019, pp. 3420–3431.

[4] P. Fiorini and Z. Shiller, "Motion planning in dynamic environments using velocity obstacles," *The International Journal of Robotics Research*, vol. 17, no. 7, pp. 760–772, 1998.

[5] A. Chakravarthy and D. Ghose, "Obstacle avoidance in a dynamic environment: a collision cone approach," *IEEE Transactions on Systems, Man, and Cybernetics - Part A: Systems and Humans*, vol. 28, no. 5, pp. 562–574, 1998.

[6] M. S. Wiig, K. Y. Pettersen, and T. R. Krogstad, "Collision avoidance for underactuated marine vehicles using the constant avoidance angle algorithm," *IEEE Transactions on Control Systems Technology*, vol. 28, no. 3, pp. 951–966, 2020.

[7] Y. Koren and J. Borenstein, "Potential field methods and their inherent limitations for mobile robot navigation," in *Proc. IEEE International Conference on Robotics and Automation*, 1991, pp. 1398–1404.

[8] A. Singletary, K. Klingebiel, J. Bourne, A. Browning, P. Tokumaru, and A. Ames, "Comparative analysis of control barrier functions and artificial potential fields for obstacle avoidance," in *Proc. IEEE/RSJ International Conference on Intelligent Robots and Systems*, 2021, pp. 8127–8136.

[9] J. Matouš, E. A. Basso, E. H. Thyri, and K. Y. Pettersen, "Unifying reactive collision avoidance and control allocation for multi-vehicle systems," in *Proc. IEEE Conference on Control Technology and Applications*, 2021, pp. 76–81.

[10] U. Borrmann, L. Wang, A. D. Ames, and M. Egerstedt, "Control barrier certificates for safe swarm behavior," in *Proc. 5th IFAC Conference on Analysis and Design of Hybrid Systems*, 2015, pp. 68–73.

[11] E. Squires, P. Pierpaoli, and M. Egerstedt, "Constructive barrier certificates with applications to fixed-wing aircraft collision avoidance," in *Proc. IEEE Conference on Control Technology and Applications*, 2018, pp. 1656–1661.

[12] L. Wang, A. D. Ames, and M. Egerstedt, "Safety barrier certificates for collisions-free multirobot systems," *IEEE Transactions on Robotics*, vol. 33, no. 3, pp. 661–674, 2017.

[13] M. Marley, R. Skjetne, and A. R. Teel, "Synergistic control barrier functions with application to obstacle avoidance for nonholonomic vehicles," in *Proc. American Control Conference*, 2021, pp. 243–249.

[14] E. H. Thyri, E. A. Basso, M. Breivik, K. Y. Pettersen, R. Skjetne, and A. M. Lekkas, "Reactive collision avoidance for ASVs based on control barrier functions," in *Proc. IEEE Conference on Control Technology and Applications*, 2020, pp. 380–387.

[15] L. Tychonievich, D. Zaret, J. Mantegna, R. Evans, E. Muehle, and S. Martin, "A maneuvering-board approach to path planning with moving obstacles," in *Proc. 11th International Joint Conference on Artificial Intelligence*, 1989, pp. 1017–1021.

[16] Z. Shiller, O. Gal, and T. Fraichard, "The nonlinear velocity obstacle revisited: the optimal time horizon," in *Guaranteeing Safe Navigation in Dynamic Environments Workshop*, 2010.

[17] D. Wilkie, J. van den Berg, and D. Manocha, "Generalized velocity obstacles," in *Proc. IEEE/RSJ International Conference on Intelligent Robots and Systems*, 2009, pp. 5573–5578.

[18] J. van den Berg, J. Snape, S. J. Guy, and D. Manocha, "Reciprocal collision avoidance with acceleration-velocity obstacles," in *Proc. IEEE International Conference on Robotics and Automation*, 2011, pp. 3475–3482.

[19] A. Chakravarthy and D. Ghose, "Collision cones for quadric surfaces," *IEEE Transactions on Robotics*, vol. 27, no. 6, pp. 1159–1166, 2011.

[20] ——, "Generalization of the collision cone approach for motion safety in 3-D environments," *Autonomous Robots*, vol. 32, p. 243–266, 2012.

[21] V. Sunkara, A. Chakravarthy, and D. Ghose, "Collision avoidance of arbitrarily shaped deforming objects using collision cones," *IEEE Robotics and Automation Letters*, vol. 4, no. 2, pp. 2156–2163, 2019.

[22] L. A. Tony, D. Ghose, and A. Chakravarthy, "Avoidance maps: A new concept in UAV collision avoidance," in *Proc. International Conference on Unmanned Aircraft Systems*, 2017, pp. 1483–1492.

[23] A. Haraldsen, M. S. Wiig, and K. Y. Pettersen, "Vehicle safety of the velocity obstacle algorithm," in *Proc. 59th IEEE Conference on Decision and Control*, 2020, pp. 5340–5347.

[24] A. Haraldsen, M. S. Wiig, and K. Y. Pettersen, "Reactive collision avoidance for nonholonomic vehicles in dynamic environments with obstacles of arbitrary shape," in *Proc. 3rd IFAC Conference on Modelling, Identification and Control of Nonlinear Systems*, 2021, pp. 155–160.

[25] ——, "Reactive collision avoidance for underactuated surface vehicles using the collision cone concept," in *Proc. IEEE Conference on Control Technology and Applications*, 2021, pp. 619–626.

[26] S. Wilson, P. Glotfelter, L. Wang, S. Mayya, G. Notomista, M. Mote, and M. Egerstedt, "The robotarium: Globally impactful opportunities, challenges, and lessons learned in remote-access, distributed control of multirobot systems," *IEEE Control Systems Magazine*, vol. 40, no. 1, pp. 26–44, 2020.

[27] M. Breivik and T. Fossen, "Principles of guidance-based path following in 2D and 3D," in *Proc. 44th IEEE Conference on Decision and Control*, 2005, pp. 627–634.

[28] E. Lalish, K. A. Morgansen, and T. Tsukamaki, "Decentralized reactive collision avoidance for multiple unicycle-type vehicles," in *Proc. American Control Conference*, 2008, pp. 5055–5061.

[29] M. S. Wiig, K. Y. Pettersen, and A. V. Savkin, "A reactive collision avoidance algorithm for nonholonomic vehicles," in *Proc. IEEE Conference on Control Technology and Applications*, 2017, pp. 1776–1783.